Efficient K-α and He-α emission from Ti foils irradiated with 400nm, 45fs laser pulses

F Y Khattak, O A M B Percie du Sert, D Riley

School of Mathematics and Physics, Queen's University of Belfast, Belfast, BT7 1NN, N. Ireland, UK

M Edwards, P Mistry, G Tallents

Department of Physics, University of York, Heslington, York, YO10 5DD, UK

P S Foster, R J Clarke, E J Divall, C J Hooker, A J Langley, D Neely, J M Smith, C Spindloe, M K Tolley

Central Laser Facility, CCLRC Rutherford Appleton Laboratory, Chilton, Didcot, Oxon., OX11 0QX, UK

Main contact email address: *f.khattak@qub.ac.uk*

Introduction

The study of K-α emission from ultra-short pulse laser produced plasmas has been pursued by several groups [see e.g. references[1-13)]]. The study of such emission can give clues to the propagation dynamics of electrons in different types of solid and as such is important in the development of schemes such as fast ignitor fusion and fast x-ray sources. Furthermore, if suitable short pulse x-ray beams can be generated then these may be used in a variety of experimental techniques, such as ultra-fast diffraction[14)] from dynamically compressed solids or x-ray scattering from non-equilibrium dense plasmas[15)].

Using fundamental laser radiation, usually at 800nm, experiments[1-13)] on a variety of target materials with pulses from 30-200fs have shown typical K-α conversion efficiencies in the range 10^{-6}-10^{-4}. Our own previous work on Astra[9)] showed peak conversion to K-α of ~10^{-4} for 800nm wavelength. However, preliminary experiments with second harmonic light[16)] showed exceptional conversion efficiency of nearly 6×10^{-4}. The pulses used were converted from the p-polarised 800nm beam by a type I KDP crystal, generating 30mJ, s-polarised pulses of ~45fs duration.

In the preliminary experiment only s-polarised data was taken and a fuller experiment was carried out as described below. The reason for taking time to mention the preliminary data is that the high yield for s-polarisation was not reproduced in the full experiment described below. The data was collected in the same way with the same spectrometer and same focusing parabola. However, there was a crucial difference in that the preliminary experiment was carried out prior to a vacuum spatial filter (VSF) being fitted to the laser and thus the focal spot quality was better in the later work. It is possible that the preliminary data had more "hot spots" in the beam and as we see below in the analysis this may be a salient point.

Experimental

Figure 1 shows the layout for the experiment. The KDP type I crystal was 0.6mm in thickness and converted up to 20% of the incident laser light to 400nm. The laser produced up to 500mJ at 800nm in 40±5 fs and tests with a calorimeter showed typically 60mJ of 400nm light on target per shot. The 400nm beam was reflected off 3 dielectric mirrors thus rejecting the unconverted ASE pre-lase and pre-pulses effectively. After reflection from a Ag mirror, the beam was focussed onto target by a Ag coated off-axis parabola (OAP) in an f/2.5 cone.

For alignment of the target an expanded green diode laser was injected through the back of the third dielectric mirror, see Figure 1. This was set to be collinear with the main 400nm beam. Because we use reflecting optics the focal spot was at the same position and in the same plane for both beams. Using a microscope objective to image the focal plane we were able to ensure that this was the case. A 10 micron wire was then inserted into the focal plane and the reflection of focal spot from this was transmitted back to the alignment system and an image of the focal spot formed on a CCD camera equipped with an objective. In this way, when the target foil was moved 1mm between shots, the position of best focus onto the foil could be identified using the very small amount of backscattered light even from smooth target surfaces. This allowed the use of angled targets and corrected for any drift in the target plane as the target moved. Leakage of 400nm light through the second dielectric was used to monitor the energy of the blue beam via a photodiode coupled to an integrating sphere with IR filtering to cut out 800nm light.

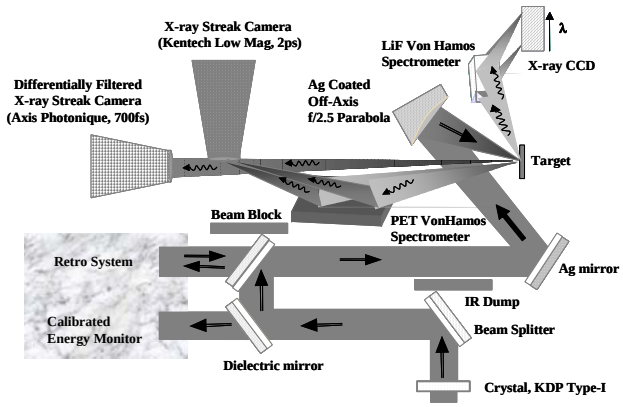

Figure 1. Schematic of the experimental arrangement.

Figure 2 shows the focal spot at best focus. This was taken at the focal position in the chamber with an objective coupled to an 8-bit CCD with the beam attenuated at the input to the compressor. The focal spot was re-optimised and tested regularly during the experiment. At best focus typically 35% of the light was contained in the central spot which was only 1.5μm x 1.9μm FWHM. At larger offsets the focal spot contained several small hot spots and the total energy was contained within the spot determined by geometrical optics.

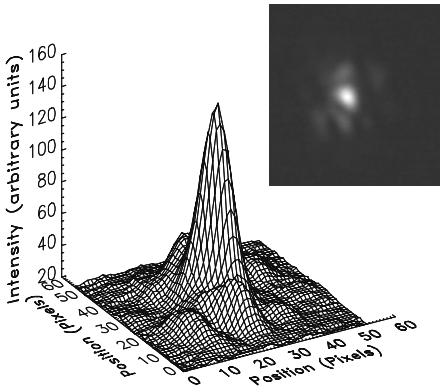

Figure 2. Image of the focal spot taken with a microscope objective and 8-bit CCD. The image was ~8x10 pixels for the central peak (1.5x1.9μm) which contained 35% of the energy with ~80% of energy contained within a 3x6.5μm ellipse.

The principal diagnostic was a von-Hamos spectrometer consisting of a LiF (200) crystal and a 16-bit CCD detector. This instrument has been previously calibrated at 5.9keV[9)] and

since in theory the reflectivity does not vary much between 4.5 and 5.9keV we used a scaled value in our data analysis. In addition to this time-integrated diagnostic we also used two X-ray streak cameras. The first was a Kentech streak using a KBr photo-cathode. With an extraction field of 22.5kV/cm and a streak rate of 2.2ps/mm we expect the resolution to be 2ps. This camera was coupled to a von-Hamos crystal which was set to record the Ti He-α line. The second streak camera was an Axis Photonique camera that uses electrostatic optics to image the slit onto the phosphor achieving 0.7ps resolution with a KI cathode[17]. This camera looked directly at the target. Ti and Sc filtering was used across the slit to show that with 12.5μm Ti filter, the camera was sensitive primarily to the K-α and He-α lines. The two streak cameras could not be used simultaneously because the Kentech interfered with the line of sight for the Axis camera.

In this experiment we were able to look at both s and p-polarisation by rotating the targets in the appropriate planes. For the case of p-polarised light we also made measurements of the specular reflection from the targets using a Molectron energy monitor. However, we were not equipped to make measurements of the light scattered in non-specular directions.

Results and Discussion

K-α and He-α yields

Figure 3 shows raw spectrometer data for two shots, one at tight focus the other at a –100μm defocus (the negative sign denotes the focus is after the target surface i.e. converging beam on target). In the first case, we see both the K-α line and strong presence of the He-α line ($1s^2$-$1s2p\ ^1P$ and satellites). In the latter case only the K-α is evident.

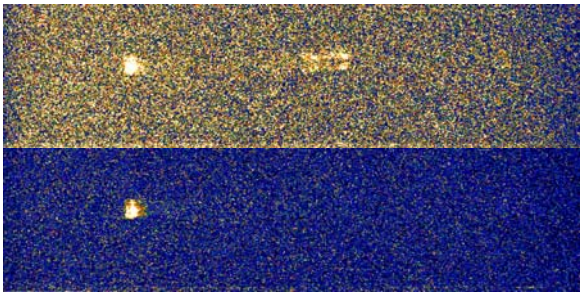

Figure 3. Two examples of the spectra obtained on single shots with the time integrated spectrometer. The grey scales are the same for both shots and as can be seen, there is considerable hard X-ray background due to fluorescence from the crystal. However, the K-α and He-α line features are clearly distinguishable.

Figure 4a shows the K-α yield for both p and s-polarised light incident at 45° on a 12.5μm thick Ti foil target as a function of offset from best focus, where positive offset means best focus is before the target plane. We can see that the yield with p-polarisation- obtained by tilting the target in the vertical plane is an order of magnitude larger than obtained with s-polarisation. Figure 4b shows the p-polarised K-α yield as a function of angle and offset. Both of these comparisons would seem to point to a resonance absorption type process or alternatively a vacuum heating[18] mechanism, we discuss this further below.

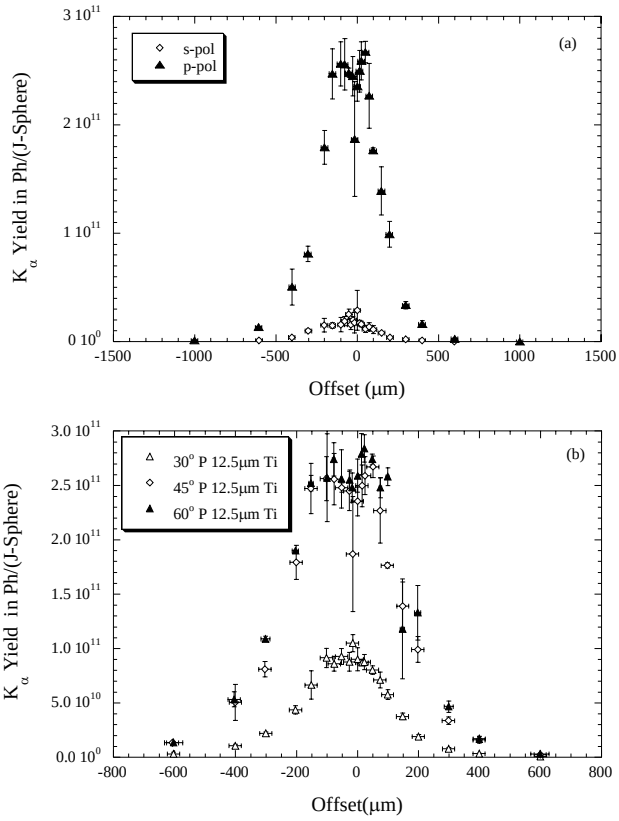

Figure 4. (a) K-α photon yield as a function of offset for 45° incidence with both s and p-polarisations. There is a clear enhancement in the latter case, indicating a resonant or quasi-resonant absorption mechanism. (b) Yield as a function of offset for p-polarisation at 30°, 45° and 60°, indicating a strong angular dependence as expected for either resonance absorption or vacuum heating. The peak yield of ~2.8×10^{11} ph/J represents a conversion efficiency for laser energy to K-α energy of ~2×10^{-4}. Each data point is the mean of at least 5 individual shots and the error bars represent the standard error in the mean.

Figure 5 shows the He-α yield for s and p-polarisation as a function of offset for 45°. As we can see there is an advantage to p-polarisation. This may be due to first, enhanced absorption for p-polarisation as shown in simulations discussed below, and/or second, such mechanisms may generate fast electrons that enhance excitation and ionisation rates in the surface plasma. As is evident, the yield for p-polarisation is comparable to that for K-α but as can be seen from the statistical error bars it is much less predictable from shot-to shot. We also note that the yield falls rapidly with offset, with a full width at half maximum of <100μm, as opposed to ~400μm for the K-α case.

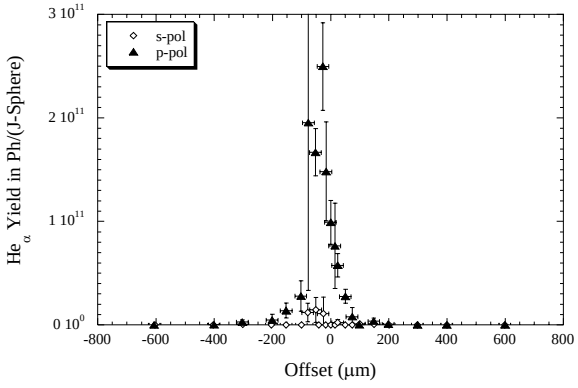

Figure 5. He-α photon yield as a function of offset for 45° incidence with both s and p-polarisations. As was the case in Figure 4(a), p-polarisation clearly favours He-α yield.

Absorption

Figure 6 shows the measured specular reflection, R, for p-polarisation, as a function of offset. It is not easy to find a simple explanation of this data because only 35% of the laser energy is in the central spot at tight focus and the spot breaks up as we move away from best focus. However, we can make some general comments. If we assume that the percentage absorption, A, is given by 100-R%, then we have high absorption (A>60%) for all cases. For the 30° data the value is roughly constant with irradiance but for 45° and 60° there is an increase in absorption close to the best focus with almost 90% implied for 60° at tight focus. This is high and it might be thought that this behaviour close to best focus is a result of non-planar expansion for a small focal spot which would lead to a lower apparent specular reflection. However, hydrodynamic simulation with the MEDUSA[19] code indicates that even if we assume that all the absorbed energy is dumped at critical density, the scale-length is still only ~0.15μm so that L/D is <0.1 where D is the FWHM focal spot.

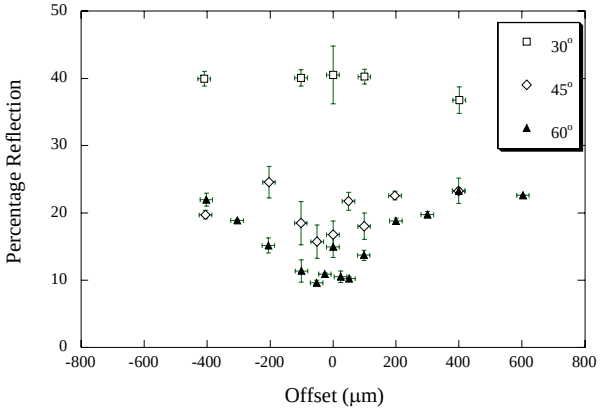

Figure 6. Specular reflection measured for p-polarisation using a molectron and the photo-diode monitor system in Figure 1b. Again each point is the mean of at least 5 shots.

Further simulations using the HYADES code[20] with a wave solver indicate that collisional absorption at the critical density surface is limited to a few percent at high irradiance and this means that the scale-length is most likely short enough that L/λ<0.1 for all the data and we are in the regime of vacuum heating rather than resonance absorption. Figure 7a shows the simulated absorption for s and p-polarisation, this is essentially collisional absorption since resonance type absorption is not calculated by the code. We can see that high absorption (~60%) is possible at high offset falling to a few percent at high intensity. This is broadly similar to the results of Price *et al.*[21] for s-polarised pulses from a similar laser. An interesting point to note is that, at low intensity, for s-polarisation the absorption falls with angle as expected but the p-polarisation case does the opposite. At high intensity all cases tend to converge to a few percent absorption.

Figure 7b shows the predicted vacuum heating absorption using the model of Brunel[18] in the relativistic regime. As we can see, from these Figures 7a and b, when we move from tight focus to the near field, the vacuum heating should fall away whilst the collisional heating should increase, perhaps explaining the flat response to offset for 30° incidence. Experimentally, for the higher angle cases, the inferred absorption is higher than for 30° even for large offsets. This may be explained by a combination of slightly higher collisional absorption (as seen in Figure 7a) and the presence of hot spots with efficient vacuum heating in the higher angle cases. As indicated above, the non-uniformity of the focal spot makes it difficult to present detailed quantitative simulations of absorption. However, it is clear that a combination of the two mechanisms can account for high absorption across all offsets and is consistent with the observed reflection.

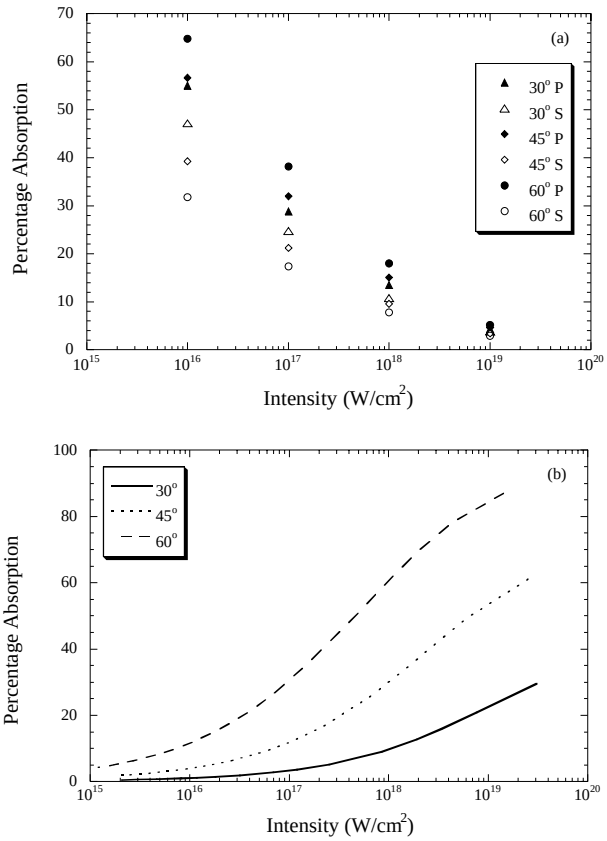

Figure 7. (a) Predicted collisional absorption for s and p-polarisation at 3 angles as given by the HYADES code. The code uses the Spitzer-Brysk model of electron ion collisions. (b) Predicted absorption due to vacuum heating for p-polarisation as given by the relativistic version of the model by Brunel. The model predicts that the temperature at the tight focus case will be ~1Mev.

Time resolved data

Figure 8 shows the time resolved emission for two experiments at p-polarised 45° irradiance on the AXIS streak camera. The targets were 1mm thick Ti foils. From tests carried out with Sc and Ti filters we know that the signal is dominated by the K-α and He-α line radiation. One experiment is at -100μm offset and the other at -200μm. These offsets where chosen as the K-α remains high but the He-α from the thermally heated plasma is now less than 1% of the K-α signal on the time integrated spectrometer. Thus the K-α dominated in both cases.

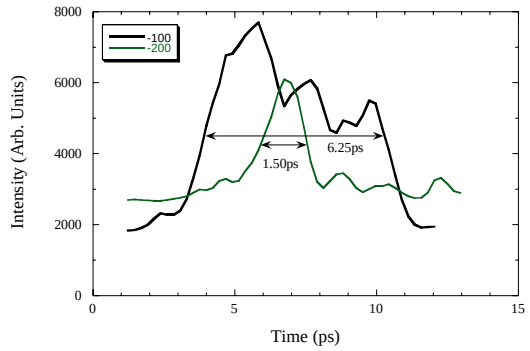

Figure 8. Time resolved emission from thick Ti foils with 45° incidence in p-polarisation. The data shown are raw line outs without deconvolution of the 0.7ps resolution or removal of the background noise in the image. The zero in the timescale is set arbitrarily.

We can see the difference made by the offset clearly in the duration of the emission. For the tighter focus we can see that the duration is of the order ~6ps with a total yield of ~2.25×10^{11} ph/J/sphere, whilst we have ~1.5ps for the lower irradiance case and a yield of ~1.3×10^{11} ph/J/sphere. Both of these times do not include the deconvolution of the ~0.7ps resolution of the camera, with the camera temporal response included we find a duration of ~1ps in the latter case and still ~6ps in the former.

This data clearly has implications for applications where it may be desired to have a very short pulse x-ray source. One of the principal advantages of laser-plasma K-α sources is that the fast electrons are only generated during the laser pulse, which can easily be sub-100fs. The fast electrons however, need to be stopped and clearly in our case they can remain in circulation for somewhat longer than the pulse width. Fast electrons that penetrate deeper into the foil than about 20-30μm should not contribute to the signal in this case as the K- α photons would be re-absorbed before escaping. Thus, we might conclude that there is some limit to the rate at which fast electrons can be injected into the foil that determines how long the K- α emission will last. It is certainly well known that there is an Alfvén limit to the current that can be sustained [e.g., see references [22, 23]] and that this along with the return current generated will be a deciding factor in the propagation of the fast electrons. The dynamics of the electrons at the surface of the target is also a factor. Whilst there are individual codes that can model different aspects of the problem, such as the generation of the fast electrons or their propagation in a solid, an understanding at present has to be gained by combining different approaches.

Figure 9 shows a streak line out taken with the Kentech camera which spectrally resolved the He-α line emission. The dynamic range was not expected to be good and the signal is weak thus only the resonance line appears to be visible above the background noise. The line out indicates that the duration of the emission is ~4ps, which corresponds to ~3.5ps if we deconvolve a 2ps resolution. Along with the data represented in Figure 5 this result indicates that for around best focus, the He-α line is roughly competitive with K-α emission in yield and duration. However, at more moderate intensity lower hard x-ray background is generated and the K-α remains efficient whilst the He-α yield drops rapidly with offset.

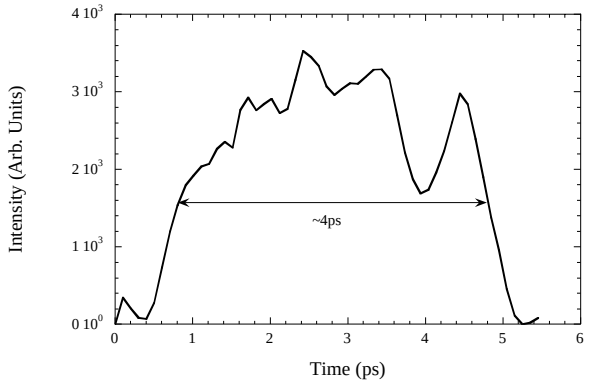

Figure 9. Time resolved He-α emission from 12.5μm thick Ti foils with 30° incidence in p-polarisation. The data shown are raw line outs without deconvolution of the 2.0ps resolution. The zero in the timescale is set arbitrarily and in this case background has been subtracted.

Conclusions

The angular behaviour of the reflected light at tight focus in the current work denotes the presence of a resonance absorption/vacuum heating type process with the latter being preferred from a consideration of the likely scale-lengths. Furthermore, high collisional absorption at modest intensity is predicted from simulations, helping to explain why reflection does not vary as much with offset in Figure 6. The picture is complicated by the fact that even outside the central spot the intensity can be high with both collisional and vacuum heating playing a role in different parts of the focal region.

Ponderomotive heating is also a possible option in high intensity interactions. This was not considered in the current data because of the angular behaviour of the K-α emission. It was considered for the preliminary data[16] which was in s-polarisation with intensity of ~10^{18} Wcm^{-2}. However, why it should be so effective in one experiment and not the other is an open question.

In summary the use of 400nm radiation has shown high conversion efficiency to K- α that is competitive with using the fundamental at 800nm. The advantages are that there is clearly a lower level of background noise associated with very hard x-rays. The time resolved data has revealed that the duration of the K-α emission is quite long in the case of tighter focus shots but can be shortened by defocusing slightly. The use of He-α as an alternative for solid foils was not seen to be very advantageous, the yield and duration were no better and tight focus with associated hard x-ray noise has to be used. In addition, the line structure would be more complex making it less monochromatic.

Acknowledgements

This work was supported under EPSRC grant EP/C001869/01.

References

1. A Rousse *et al.*, Phys Rev E 50,2200 (1994)
2. C Reich *et al.*, Phys.Rev.Lett. 84, 4846 (2000)
3. D C Eder *et al.*, Appl.Phys.B 70, 211 (2000)
4. K B Wharton *et al.*, Phys Rev E 64, 025401 (2001)
5. T Feurer *et al.*, Phys Rev E 65, 016412 (2002)
6. D Salzmann *et al.*, Phys Rev E 65, 036402 (2002)
7. C Ziener *et al.*, Phys Rev E 65, 066411(2002)
8. F Ewald *et al.*, Europhys.Lett. 60, 710 (2002)
9. F Y Khattak *et al.*, J.Phys.D 36, 2372 (2003)
10. K B Wharton *et al.*, Phys. Rev. Lett. 81,822 (1998)
11. M Hagedorn *et al.*, Appl. Phys. B 77,49 (2003)
12. F Pisani *et al.*, Appl.Phys.Lett. 84, 2772 (2004)
13. H Nishimura *et al.*, J. Quant. Spectrosc. Radiat. Transfer 81, 327 (2003)
14. C Rose-Petruck *et al.*, Nature 398, 310 (1999)
15. E Nardi *et al.*, Phys Rev E 57, 4693 (1998)
16. F Y Khattak *et al.*, RAL-TR-2004-025,55 (2004)
17. P Gallant *et al.*, Rev. Sci. Instr. 71, 3627 (2000)
18. F Brunel, Phys. Rev. Lett. 59, 52 (1987)
19. J P Christiansen *et al.*, Computer Phys. Comm.7, 271 (1974)
20. J T Larsen J T and S M Lane, J. Quant. Spectrosc. Radiat. Transfer 51, 179 (1994)
21. D F Price *et al.*, Phys. Rev. Lett. 75, 252 (1995)
22. A R Bell *et al.*, Plasma Phys.Controlled Fusion, 39, 653 (1997)
23. J R Davies *et al.*, Phys Rev E., 56, 7193 (1997)